

Minimizing interferometer misalignment errors for measurement of sub-nanometer length changes

R. Schödel*, Arnold Nicolaus and G. Bönsch

Physikalisch-Technische Bundesanstalt (PTB), Braunschweig, Germany

ABSTRACT

The detailed knowledge of thermal expansion and dimensional stability of low expansion materials is of growing interest and requires measurements of length changes with sub nm uncertainty. In addition to accurately defined environmental conditions the interferometer adjustment, namely the number of fringes covering the sample and also the method of autocollimation adjustment, become more important. Their influence, investigated with PTB's precision interferometer, will be discussed.

1. INTRODUCTION

Demands on dimensional stability and on the detailed knowledge of thermal expansion properties of "high tech" materials are growing considerably from year to year. One application is the further development of photolithography towards the so called EUV – Lithography using 13 nm as light source. At this wavelength mirrors are used as main optical components. Therefore it is very important to know the geometrical properties of the substrates at different temperatures.

These properties can be investigated by observing length changes of macroscopic samples as a function of temperature, time and also pressure. For this purpose special interferometers of different types can be used: i) interferometric dilatometer [1], ii) high-finesse Fabry–Perot interferometer [2], and iii) sophisticated Twyman-Green interferometer [3] as the PTB precision interferometer from this study.

Although ii) provides the best resolution according to ultra high resolvable frequency changes, the method iii) has distinct advantages: the "length topography" can be observed so that, in addition to a single value assigned to the length, bending of the sample or topography changes can be monitored. Furthermore, measurements can be performed in vacuum but also at a defined air pressure. Finally, iii) is based on the measurement of the absolute length of the sample so that the measurements can be continued after samples are replaced.

This paper focuses onto latest improvements of the PTB precision interferometer for observing lowest length changes.

2. EXPERIMENTAL SETUP

2.1. Description of the Interferometer

Fig. 1 shows the interferometer situated in a temperature controlled chamber and by a vacuum tight environmental chamber. Two measurement modes are possible: i) measurements under air pressure where a constant and defined pressure is provided by a pressure balance (assembled and calibrated at PTB), ii) measurements in vacuum (< 0.1 Pa) where a turbo pumping unit is connected to the chamber.

The interferometer is equipped with three PTB-made stabilized lasers at 780 nm (Diode, Rb-stabilized), 633 nm (He-Ne, I₂-stabilized) and 532 nm (frequency doubled Nd:YAG, I₂-stabilized) where the latter is considered as the most stabile (long time stability better than 10^{-12} [4]).

The laser light passes (alternatively) a 200 μ m multimode fibre which represents the entrance of the interferometer at the focal point of the collimator (600 mm focal length). The reference path of the interferometer can be varied for phase stepping by slightly tilting the compensation plate. The tilt angle is monitored by an auxiliary interferometer and servo controlled [5]. For measurements in air the measuring path contains a 400 mm vacuum cell close to the sample to determine the refractive index of air at the specific environmental conditions. The surface temperature of the sample is

* rene.schoedel@ptb.de; phone: +49 531 592 5411; fax: +49 531 592 4305; Physikalisch-Technische Bundesanstalt (PTB); section 5.41, Bundesallee 100, D-38116 Braunschweig

measured by thermo couples near the front face and near the wrung platen with an uncertainty < 1 mK (described in [6]).

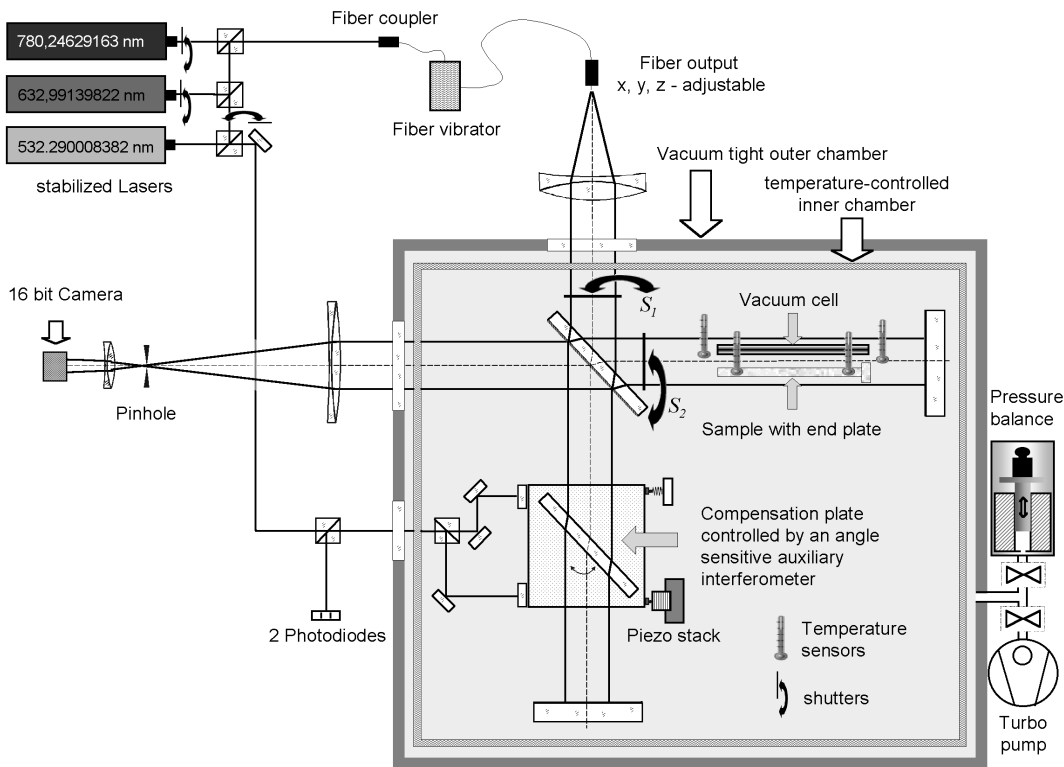


Figure 1 Experimental setup (see text for details).

Small wedges of the optical flats prevent multiple reflections that would interfere with the main beams and disturb the interference pattern. The pinhole at the interferometer output blocks unwanted reflections and is also necessary for the adjustment of the interferometer.

The interference pattern is evaluated by phase stepping interferometry as described in [7]. Instability of the interferometer can easily be recognized by comparison of the phase topographies derived from two different data sets.

A 512×512 pixel camera system (Photometrics CH 350) provides 16-bit data frames. Fig. 2 shows the array of interference phase data of a typical sample wrung to a platen. The data in the regions P_{left} , P_{right} on the platen, and S on the sample front face are used for the evaluation of the interference fraction and finally the length. Deviations from ideal parallelism (mainly appearing along the i -direction) and also surface texture require a most accurate definition of the regions. Also a length correction for sub-pixels is necessary as it is outlined in detail in [5]. The phase steps between platen and sample, investigated within E_{left} and E_{right} in fig. 2 are used for the definition of an edge array (fig. 2, right). The data in the edge arrays are used to identify the position of the phase steps between platen and sample and a straight line is fitted. The uncertainty of this procedure is typically lower than 5% of a pixel. Because this method is applied at both edges, the final uncertainty of the central position (marked by +) in i -direction is better than 0.03 pixels. This permits an accurate assignment of the regions P_{left} , P_{right} and S to the camera pixels. Because of the camera resolution the uncertainty of the central position of the 9×27 mm sample along i is about $3 \mu\text{m}$. For the samples used, a possible dependence of the length from the j -position can be neglected.

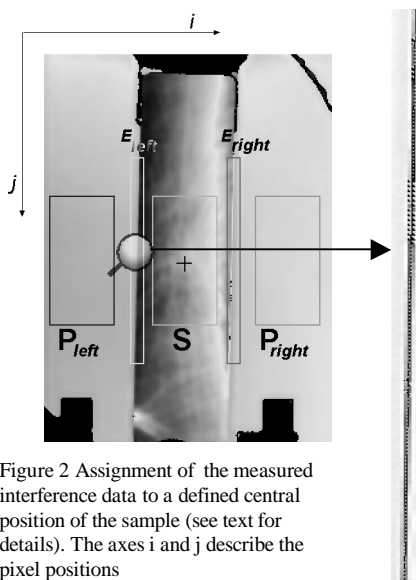


Figure 2 Assignment of the measured interference data to a defined central position of the sample (see text for details). The axes i and j describe the pixel positions

2.2. Autocollimation adjustment procedure

Autocollimation misalignment can be regarded as one of the major uncertainty contributions in interferometric length measurement via the so called cosine error also termed “obliquity error” [8]. Fig. 4 shows the course of light beams when the fibre end is displaced by an amount of δ from the optical axis corresponding to a misalignment angle of $\alpha \approx \delta/f_{\text{collimator}}$ of the interferometer where the focal length, $f_{\text{collimator}}$, of the collimator used in the precision interferometer is 600 mm. A displacement of 60 μm would result in $\alpha \approx 10^{-4}$ rad and the cosine error ($1-\cos \alpha \approx \alpha^2/2$) amounts to 5×10^{-9} . The measurement of a 200 mm sample therefore would lead to a result that is 1 nm to short.

The application of a microscope at the output pinhole of the interferometer together with an appropriate autocollimation illumination source can be very helpful. However, the quality of such a interferometer alignment procedure depends on the properties of the used observation optics and also the “operators eyes”. Furthermore it requires the optics at the interferometer output (see fig. 1) to be switched to this adjustment mode.

Boensch [9] used autocollimation adjustment method using a mono-mode fibre for most precise wavelength comparison. Lewis and Pugh [10] used a similar method using a bundle of single-mode optical fibres. Each fibre (with a diameter of about 10 μm) could be used either as source fibre or for detecting the return spot of the interferometer. As outlined in [10], the use of single-mode fibres over multi-mode fibres has advantages mainly regarding the absence of speckles caused by mode mixing in multi-mode fibres. In spite of this benefit together with the small diameter mono-mode fibre cause problems according to our observations: the fully spatial coherence causes disturbing interferences which are difficult to distinguish from the “normal” interference pattern. These disturbing interferences which might be caused by slight reflections on spherical surfaces were found to be up to 1/20 interference order, strongly dependent on the distance of the mono-mode fibre from the collimator. Furthermore, mono-mode fibres can only be used in a restricted wavelength band.

For these reasons, at the precision interferometer a multi-mode fibre is used together with a fibre vibrator (see fig. 1) removing speckle noise very effectively. This same fibre is used for all three wavelengths. The principle of autocollimation adjustment is similar to [9] where the fibre end at the entrance of the interferometer is moved and the back reflex of the reference mirror is recorded. The same fibre is used as light source as well as for detecting the back reflex at closed measuring path of the interferometer (shutter S_2 in fig.1 is closed). The return signal is extracted via a beam splitter close to the entrance of the fibre (see fig. 3). Signal contributions from light reflections at the two faces of the fibre are measured as offset when the shutter is closed. A computer controlled translation stage (VT-80, MICOS GmbH, Germany) is used to move the fibre in a plane perpendicular to the optical axis (in xy-direction). The axial position (z) has to be set manually. A PC-program reads the signal data of the back reflection at a certain position of the fibre.

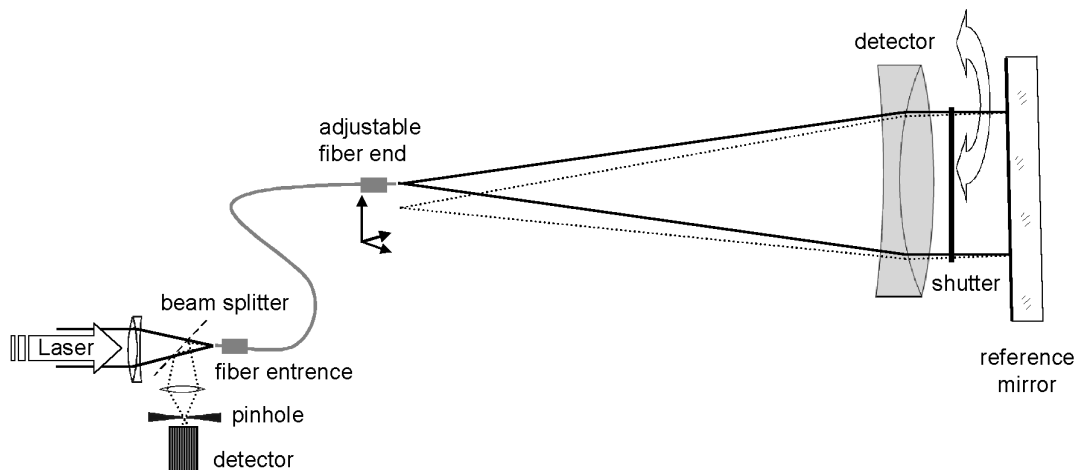


Figure 3
Autocollimation
setup used at the
precision
interferometer

The signal of back reflected light from the interferometer is scanned as a function of x and y at a specific z -position. From these data, read at a rate of about 10 Hz, the centre (x_c, y_c) can be calculated according to the following equation:

$$(x_c, y_c) = \frac{\sum_{n=1, m=1}^{N, M} (x_n, y_m) \times [S(x_n, y_m) - S_0]}{\sum_{n=1, m=1}^{N, M} [S(x_n, y_m) - S_0]}, \quad (1)$$

where $S(x_n, y_m)$ is the measured detector signal at the position (x_n, y_m) , S_0 the offset signal measured with the shutter closed and N, M the number of steps in x - and y -direction, respectively. This definition of the centre is much more accurate than simply searching the maximum value of $S(x_n, y_m)$. In a next step the translation stage is set to the determined central position which is then assigned to $(x, y) = (0, 0)$. A second scan is performed in order to check that this zero position is confirmed as centre of the spot according to eq. 1. The z -coordinate is varied in order to find the optimum position in the focal plane.

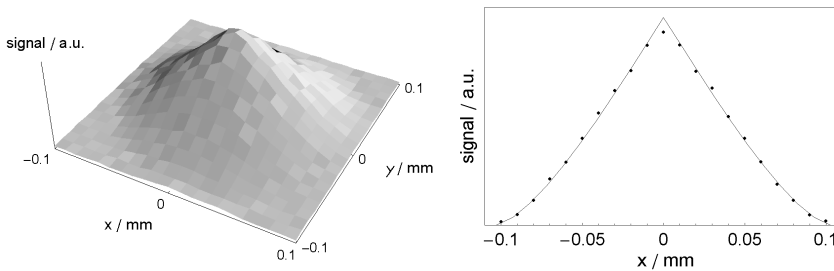


Figure 4 Interferometer back reflection signal as a function of x and y (left) The right plot shows a section in x -direction together with a theoretical curve (solid line for details, see text).

Fig. 4, left side, shows the result of the second scan where S_0 is already subtracted. Fig. 4, right side shows a section in x -direction at y_c together with a theoretical curve (solid line) calculated from the overlap of two circles areas as a function of the displacement. Obviously there is a good agreement between the measurement and the expected function at the optimum z position. The diameter of the assumed circles was varied for the best fit resulting in a value of $208 \mu\text{m}$. This result matches well with the fibre diameter of $200 \mu\text{m}$ specified by the manufacturer and gives evidence for the quality of the method described.

Deviations of the central position found from scan to scan are typically well below $5 \mu\text{m}$. This is much smaller than expected according to the specifications of the manufacturer of the xy -stage.

3. CHARACTERIZATION OF THE PRECISION INTERFEROMETER BY MEASUREMENTS

The performance of the precision interferometer was investigated and systematic influences of the adjustment were studied with measurements performed at a 200 mm sample under vacuum conditions ($< 0.1 \text{ Pa}$). To separate length changes due to temperature, a ULE-glass sample (Corning Coop.) was used and the measurements were performed at about $20 \text{ }^\circ\text{C}$, near the zero crossing point of the sample's thermal expansion coefficient (found near 17°C).

3.1. Length deviations related to the use of different wavelengths

The precision interferometer uses three wavelength of different stabilized lasers. The sample lengths obtained with the three wavelength should be identical unless there are other effects.

Fig. 5A shows that the spread between the measured length is more than 1 nm which seems large. However, a closer look to the data reveals that the sample edge position (see fig. 2) is slightly dependent on the wavelength used. The difference between the green and the nir-edge is approximately one half a pixel corresponding to about $50 \mu\text{m}$ caused by chromatic aberration. Usually the computer program detects the edges at each wavelength and uses average edge positions for the length evaluation. On the other hand, the shift of the evaluated area by $50 \mu\text{m}$ can be responsible for a different length value. In fact, the used sample is out of parallelism by 2.40 nm per Pixel in i -direction ($\approx 20 \text{ nm}$ per

mm = 20 μ rad) what can explain this effect. In order to check this hypothesis the length evaluation at each wavelength was temporary modified so that individual found edges were used. The result of this procedure is shown in fig. 5B. It turns out that the agreement is considerably improved to about ± 0.2 nm. However, the mean value of the three lengths, indicated by the thick black lines in fig. 5, is the same (within 0.01 nm) regardless whether the position of the areas are determined individually for each wavelength or an average position is used for the evaluation.

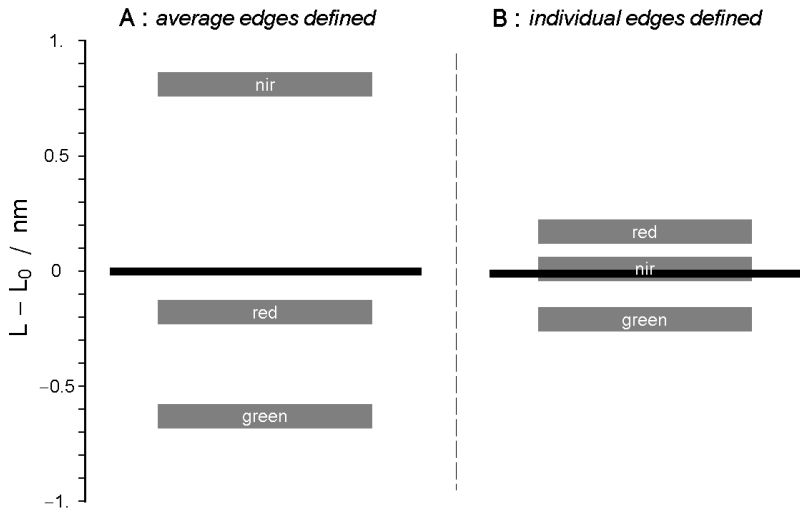


Figure 5 Spread of lengths data (grey areas), obtained with the three stabilized laser wavelength, around the mean length $L_0 = 200.01519197$ mm (thick black line).
 A: average edge positions were used for length evaluation
 B: individual edge positions found at the specific wavelength were used

The sensitivity of the evaluated length in j-direction found for this specific sample is much less (≈ 0.01 nm per pixel). This was observed for the majority of samples and seems to be caused by sample manufacturing process.

3.2. Influence of fringe adjustment on length evaluation

Usually the measurements with the precision interferometer are performed in fluffed out mode where the wave fronts of the reference beam and the beam reflected from the sample have exact the same direction which is adjusted by autocollimation (see 3.1.). In this way the sample- and platen-surface can be assumed to be perpendicular to the optical axis so that there is no “cosine error” (despite of the constant influence originating from the aperture size [8] which is not relevant when length changes, as discussed here, are in the focus of interest).

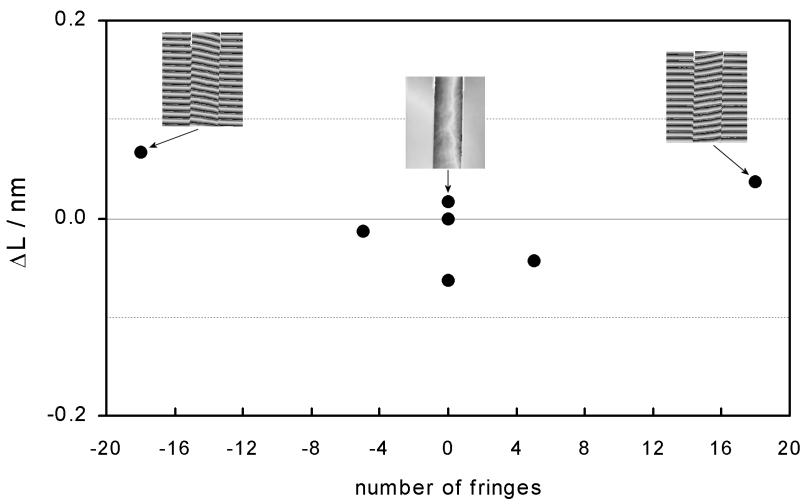


Figure 6 Length evaluation at different vertical tilts of the interferometer reference mirror (given in units of the number of fringes covering the sample). The sample- and platen-face is perpendicular to the optical axis defined by autocollimation. The inserts illustrate the mode of interference pattern. The same 200 mm sample was used as in fig. 5.

A tilt of the interferometer reference mirror causing fringes in the interference pattern should therefore not influence the measured length. Various measurements were performed at different tilt angles of the reference mirror. In order to

minimize the measuring time, the investigation was performed with the green laser. The results presented in fig. 6 clearly show that a tilt of the reference mirror does not influence the measured length within 0.1 nm.

3.3. Influence of autocollimation adjustment

In the following section the sensitivity of the length measurement on specific misalignments is investigated. At first the influence of the axial position was studied. The fibre was displaced from an optimum z-position by a certain amount before the autocollimation adjustment procedure (see 3.1.) was applied and the measurement was performed. Fig. 7 shows the results of several measurements using the green laser wavelength.

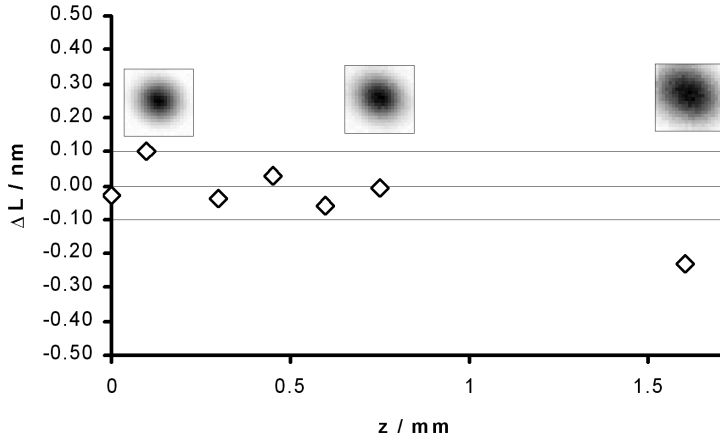


Figure 7 Length evaluation at different axial (z-)positions of the fibre. Autocollimation was performed after z was set. The inserts show the corresponding scan as density graphics (compare fig. 4). The optimum z-position was assigned to zero.

The same ≈ 200 mm sample was used as in fig. 5.

The deviations of the data from an average shown in Fig. 7 are not larger than 0.1 nm as long as the misalignment of z does not exceed large values (>1 mm). Even the -0.2 nm length deviation of the point of the right side in fig. 7 may be caused by insufficient xy-adjustment due to a too small scan area. Therefore adjustment with respect to the z-position of the fibre end is not critical.

As it was discussed in 3.2., autocollimation means that the optical axis is perpendicular to the sample front face and the platen, respectively. Therefore, there are two ways to alter the adjustment in a defined way: i) setting a tilt of the sample with respect to the reference mirror which remains perpendicular to the optical axis, ii) defined displacement of the fibre in the xy-plane from the zero (autocollimation) position.

The misalignment angle α can be calculated in each case resulting in a corresponding “cosine error” expected at the 200 mm sample used for the measurements. In case i) α is obtained from the variation of the interference phase, derived from the unwrapped phase interval at the wavelength used, related to the size d in a continuous sample area (in which this phase interval was found):

$$\alpha = \frac{\lambda}{2} \left(\frac{\Phi_{\max}}{2\pi} - \frac{\Phi_{\min}}{2\pi} \right) / d \quad (2a)$$

In case ii) α is derived simply from:

$$\alpha = \arcsin(\delta / f_{\text{collimator}}) \cong \delta / f_{\text{collimator}} \quad (2b)$$

where δ is the amount of displacement from the optimum zero- xy-position and $f_{\text{collimator}}$ the focal length of the collimator (600 mm).

At a given sample length L , the expected length deviation is obtained from:

$$\Delta L = L \times (\cos \alpha - 1) \cong -L \times \frac{\alpha^2}{2} \quad (3)$$

Fig. 8 shows the measured length change derived as a function of the sample tilt angle for the case of vertical fringes. The solid line indicates the expected cosine error according to eqs. 2a and 3. As it is drawn on the top of fig. 8, the deviations of the measured data from the expected length change is very small. The same result was obtained when the position of the fibre was changed in x-direction (same angle orientation as in fig. 8) and the length was measured in fluffed out mode. This is shown in fig. 9 where the expected cosine error was calculated according to eqs. 2b and 3.

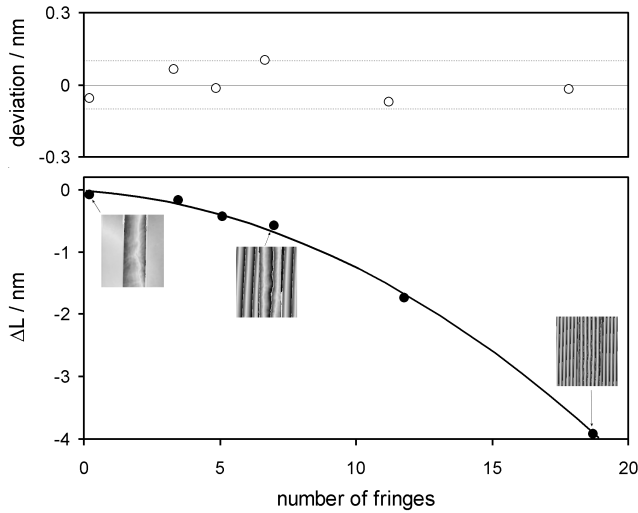


Figure 8 Length evaluation at different sample tilts causing vertical fringes. The tilt is with respect to the reference mirror that was adjusted by the described autocollimation procedure. For illustration interference pattern are inserted. The same 200 mm sample was used as in fig. 5.

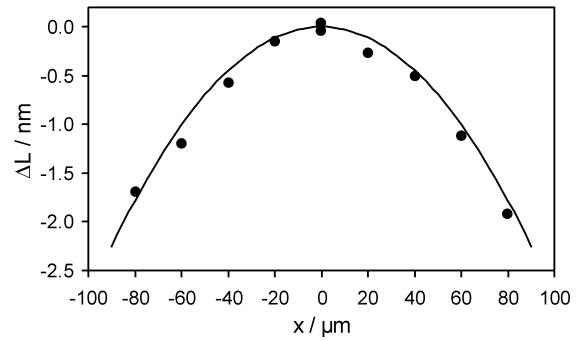


Figure 9 Length evaluation at different x-positions of the fibre.

A variation of the length was also observed when the sample is tilted so that horizontal fringes are observed. Fig. 10 shows the measured length change as a function of the number of horizontal fringes.

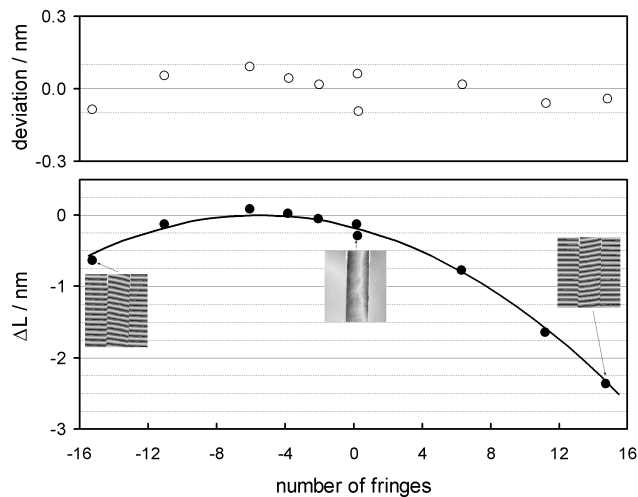


Figure 10 Length evaluation at different sample tilts causing horizontal fringes. The same 200 mm sample was used as in fig. 5.

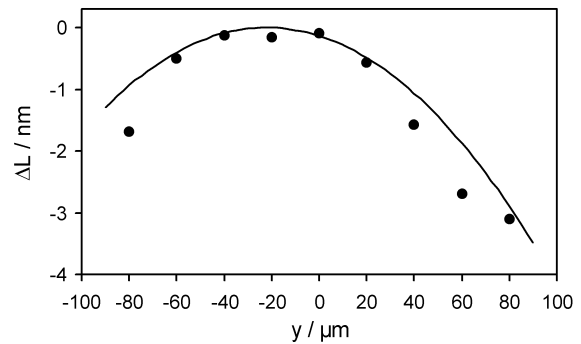


Figure 11 Length evaluation at different y-positions of the fibre.

Obviously the maximum length is shifted and can be found near minus five fringes. If an angle shift corresponding to this amount is taken into account, the measured data correspond well with the solid line in fig. 10 and the length deviations drawn on the top of fig. 10 become small. A similar observation was made as the position of the fibre was changed in y-direction (same angle orientation as in fig. 10) and the length was measured in zero fringe mode: the shift of the solid line by $-25 \mu\text{m}$ shown in fig. 11 corresponds to the same offset angle ($\approx 40 \mu\text{rad}$) as in fig. 10. These results were found to be reproducible. The explanation for the shift of the centre is given as follows: the scan is performed in the way that, after the x- position of the translation stage was set, the signals along the y-axes are read. Since the data rate is about 10 Hz the length of stay at a certain y-position is relatively short. Therefore a drift of the y-position is conceivable. The direction of the effect (negative sign, see fig. 11) supports this idea and also explains why such an effect was not found in x-direction.

The above shift of $25 \mu\text{m}$ corresponds to a “cosine error” of less than 0.15 nm which would be constant because the shift was found to be reproducible and therefore would not affect the measurement of length changes. However this is valid only for measurements in zero fringe mode. If for example the measurement would be performed once at plus five fringes and some other time at minus five fringes, a length change of about 0.5 nm would be pretended. Thus, measurements in fluffed out mode and preceding autocollimation adjustment as described in this paper are the best prerequisite for most precise measurements.

4. MEASUREMENT EXAMPLES

The measurements shown in chapter 3. were all performed under most stable conditions combined with a relatively short time interval. The spread found in the data was usually within $\pm 0.1 \text{ nm}$. The uncertainty of measurements performed with the precision interferometer of course can be expected to be higher. It is difficult to speculate about uncertainties in this sub-nm range where smallest (also unknown) disturbances can affect the measurement results. Therefore here only two examples of measurements are presented without detailed discussion which demonstrate the obtainable accuracy.

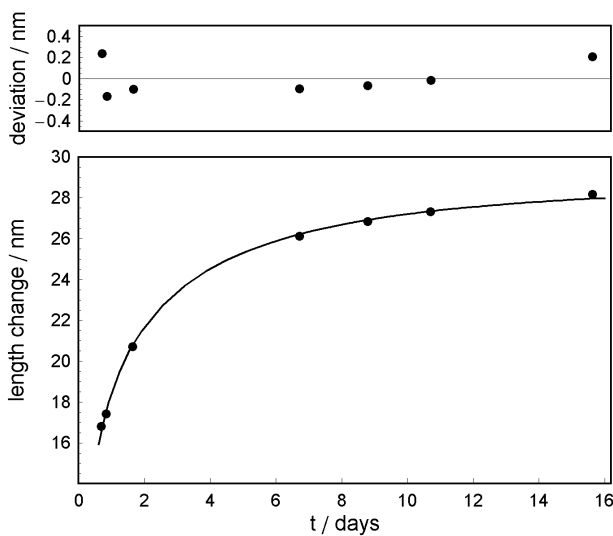


Figure 12. Length relaxation of a Zerodur sample at constant temperature of 30°C following a temperature step from 20°C to 30°C

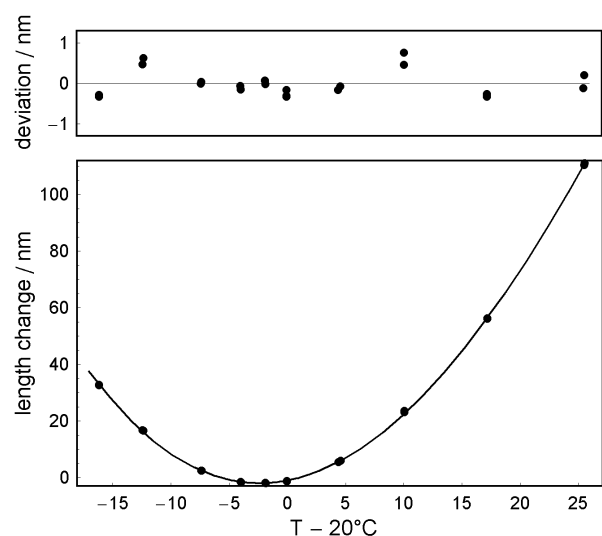


Figure 13. Thermal expansion measurements at a ULE- sample

The measurements depicted in fig. 12 are performed at constant temperature over a time period of almost three weeks. They show the length relaxation of a Zerodur sample following a temperature change from 20°C to 30°C (see [11]) together with a hypothetical fit function (solid line). The data points on the top show the deviation from the relatively smooth fit curve. These deviations are about $\pm 0.2 \text{ nm}$ in maximum.

In the case of fig. 13 the dependence of the length from the temperature of the ULE sample used in chapter 3. is shown. Length relaxation of this sample which could affect the data in this diagram was not observed. However, the deviation from a smooth fit curve is somewhat higher with maximum values of about 0.5 nm. Most likely this discrepancy does not originate from a more complicated thermal expansion behaviour. We address this effect to a possible temperature influence to the optics of the interferometer which should be investigated in more detail in future studies.

5. CONCLUDING REMARK

The improved precision interferometer described and investigated in this paper seems to have the potential for reliable measurements in the sub-nm range. This was demonstrated by measurements, where the influence of the interferometer adjustment was investigated carefully. Although the measurement examples reveal a slightly increased uncertainty compared to the < 0.1 nm spread found at the test measurements, the instrument described seems to be a very good tool for most precise measurements of length changes.

REFERENCES

1. M. Okaji and H. Imai 1992. Development of an interferometric dilatometer with optical heterodyne system. *Netsu Bussei* 6:83-8.
2. F. Riehle. Use of optical frequency standards for measurements of dimensional stability. *Meas. Sci. Technol.* 9:1042-1048 (1998)
3. Schödel, R. and Bönsch, G. Interferometric measurements of thermal expansion, length stability and compressibility of glass ceramics, Proceedings of the 3rd International Conference [and 4th General Meeting of the] European Society for Precision Engineering and Nanotechnology: 2 (2002), 691 – 694. ISBN: 90-386-2883-8.
4. P. Cordiale, G. Galzerano and H. Schnatz. International comparison of two iodine-stabilized frequency-doubled Nd:YAG lasers at 532 nm. *Metrologia* 37, 177-182 (2000)
5. Schödel, R. and G. Bönsch 2001. Precise interferometric measurements at single crystal silicon yielding thermal expansion coefficients from 12 °C to 28 °C and compressibility. *Proc. SPIE* 4410:54-62.
6. G. Bönsch, H.-J. Schuster, R. Schödel. High-precision temperature measurements with thermo couples. *Technisches Messen*: 68, 550 - 557 (2001)
7. R. Schödel, A. Nicolaus and G. Bönsch. Phase stepping interferometry: Methods for reducing errors caused by camera nonlinearities. *Appl. Opt.* 41, 55 - 63 (2002)
8. Bruce, C.F. The effects of collimation and oblique incidence in length interferometers. *Aust. J. Phys.* 8, 224-240 (1955)
9. G. Bönsch. Simultaneous wavelength comparison of iodine stabilized lasers at 515 nm, 633 nm, and 640 nm. *IEEE Transactions on instrumentation and measurement*, Vol. IM34: 248-251 (1985)
10. Lewis, A. and D.J. Pugh. Interferometer light source and alignment aid using single-mode optical fibres. *Meas. Sci. Technol.* 3 929-930 (1992).
11. Schödel, R. and Bönsch, G. Interferometric measurements of thermal expansion, length stability and compressibility of glass ceramics, Proceedings of the 3rd International Conference [and 4th General Meeting of the] European Society for Precision Engineering and Nanotechnology: 2 (2002), 691 – 694. ISBN: 90-386-2883-8.